Separation of mycolic acid isomers by cyclic ion mobility-mass spectrometry

DE LAS HERAS PRIETO, Hector, COLE, Laura <http://orcid.org/0000-0002-2538-6291>, FORBES, Sarah <http://orcid.org/0000-0002-8361-6390>, PALMER, Martin and SCHWARTZ-NARBONNE, Rachel <http://orcid.org/0000-0001-9639-9252>

Received: 31 July 2024 | Revised: 11 September 2024 | Accepted: 12 September 2024

DOI: 10.1002/rcm.9917

RESEARCH ARTICLE

Rapid Communications in Mass Spectrometry WILEY

Separation of mycolic acid isomers by cyclic ion mobility-mass spectrometry

Hector de las Heras Prieto[1] | Laura M. Cole[1] | Sarah Forbes[1] | Martin Palmer[2] | Rachel Schwartz-Narbonne[1]

[1]Biomolecular Research Centre, Sheffield Hallam University, Sheffield, UK

[2]Waters Corporation, Wilmslow, UK

Correspondence
Rachel Schwartz-Narbonne, Biomolecular Research Centre, Sheffield Hallam University, Sheffield, UK.
Email: r.schwartz-narbonne@shu.ac.uk

Funding information
Community for Analytical Measurement Science; Analytical Chemistry Trust Fund

Rationale: Mycobacterial species contain high concentrations of mycolic acids in their cell wall. Mycobacteria can pose a threat to both human health and the environment. Mass spectrometry lipidomic characterization can identify bacterial species and suggest targets for microbiological interventions. Due to the complex structures of mycolic acids and the possibility of isobaric isomers, multiple levels of separation are required for complete characterization. In this study, cyclic ion mobility (cIM) mass spectrometry (MS) was used for the analysis, separation and fragmentation of mycolic acids isomers from the bacterial species *Gordonia amarae* and *Mycobacterium bovis*.

Methods: Mycolic acid isomers were interrogated from cultured *G. amarae* biomass and commercially available *M. bovis* mycolic acid extracts. These were infused into a cIM-enabled quadrupole time-of-flight MS. Ions of interest were non-simultaneously selected with the quadrupole and passed around the cyclic ion mobility device multiple times. Fragment ion analysis was then performed for the resolved isomers of the quadrupole-selected ions.

Results: Repeated passes of the cIM device successfully resolved otherwise overlapping MA isomers, allowing isomer isolation and producing an ion-specific post-mobility fragmentation spectrum without isomeric interference.

Conclusions: Mycolic acids (MA) isomers from *G. amarae* and *M. bovis* were resolved, resulting in a high mobility resolution and low interference fragmentation analysis. These revealed varying patterns of MA isomers in the two species: *G. amarae's* most abundant ion of each set of MA has 1–2 conformations, while the MA + 2 *m/z* the most abundant ion of each set has 3–6 conformations. These were resolved after 70 passes of the cyclic device. *M. bovis'* most abundant ion of each keto-MA set has 2 conformations, while the keto-MA + 2 *m/z* has 1–2 conformations. These were resolved after 75 passes.

1 | INTRODUCTION

1.1 | Mycobacteria and mycolic acids

The genus *Mycobacterium* encloses more than 190 species that contain high concentrations of mycolic acids in their cell walls.[1] Certain mycobacterial species are human pathogens; for example, *Mycobacterium bovis* is the causative agent of tuberculosis, which has a high mortality if left untreated.[2] Other non-pathogenic mycobacteria, such as *Gordonia*, are associated with environmental issues. For example, *Gordonia amarae* is a known contributor to foaming events in activated sludge (AS) reactors of wastewater treatment plants, producing biosurfactants that alter the process efficiency[3] and consequently, leading to environmental contamination by the release of non-properly treated wastewater into the environment.

Mycolic acids (MA) are long-chain fatty acids found in the two outer mycobacteria membrane leaflets, including trehalose mono/di-mycolate and glucose monomycolate.[4] These are composed of an alkyl side chain and a hydroxyl group (2-alkyl, 3-hydroxy)[5] and can be covalently or non-covalently bound to the mycobacterial cell wall,[5] providing essential functions in the biosynthesis and permeability of the wall. Although MA are structurally unique, they are not exclusive to mycobacteria, being found in other related genera such as *Nocardia*, *Rhodococcus* and *Corynebacterium*.[4] The main classes of MA in mycobacteria are alpha-, keto- and methoxy- MA.

MA in *M. bovis* provide mechanical support, osmotic protection and contributes towards both antimicrobial resistance[6] and immune recalcitrance through supporting bacterial survival inside macrophages.[7] Since they are also essential in the pathogenicity of the bacteria, the MA biosynthesis path has been targeted as an action site of anti-TB drugs and for the wider development of antimycobacterial drugs.[8] MA in *Gordonia* is mostly constituted of an even number of carbon chain lengths with a total number of carbon atoms ranging from 40 to 66. They typically have between 0 and 5 double bonds or unsaturations,[9] however, this is strain dependent. Lipidomic analysis is therefore a powerful technique to identify bacterial species[10] and to identify targets for lipid-based treatments.[8] Previous studies show considerable interest in elucidating MA isomers employing ion mobility,[11] however, to date, cIM has not been applied to this question. cIM therefore has the potential to provide an improved method for the identification, isolation and fragmentation of MA isomers.

1.2 | Cyclic ion mobility (CIM)

Ion mobility separation (IMS) is a powerful technique; when coupled with a mass spectrometer it allows the possibility of a multidimensional characterization of the analytes,[12] providing further separation of isobaric species. There is a wide range of IMS systems with different modes of operation such as drift tube ion mobility spectrometry (DTIMS), trapped ion mobility spectrometry (TIMS), travelling wave ion mobility spectrometry (TWIMS), field asymmetric waveform ion mobility spectrometry (FAIMS), etc.[12] TWIMS was introduced in 2006 by Waters Corporation[13] and has been further developed to the modern cyclic ion mobility systems.

cIM provides selectable mobility resolution and permits experiments combining numerous functions such as mobility selection, ion storage and IMS^n.[14] The cIM is designed as a quadrupole/cyclic ion mobility/time-of-flight instrument which uses travelling waves (TWs) for mobility separation in a closed loop region.[14] Ions that enter the cIM section "surf" on a wavefront, while waves that are passing through the section repeatedly overtake them. The mobility of the ions determines how frequently they are surpassed by the waves, with lower mobility ions being overtaken more frequently and taking longer to traverse the section than higher mobility ions, leading to IM separation.[14]

The cIM device consists of an entry/exit array situated at the bottom of the cIM loop in the middle of a pre- and post-array ion store areas which makes possible a wide range of ion mobility sequences.[15] Ion packets coming from the trap are held in the array until a change in voltage allows them to enter the cyclic section where IM separation occurs.[14] After separation ions can be ejected directly to the post-array store and then to the ToF analyser. Data acquisition can be triggered or not depending on the experimental aim. Other ejection functions can be applied such as IMS^n, where multiple isomers can be resolved for a single ion; individual mobility-separated isomers of interest are ejected back to the pre-array store and held while the rest get ejected to ToF without acquiring. Stored ions can then be re-injected to the cyclic section with or without activation and further separation/ejection steps can be selected, allowing the possibility of IM separation of fragment ions (if activation was selected) and further fragmentation of selected fragment ions and so on. Most of these functions were used for data acquisition in this project.

2 | EXPERIMENTAL

2.1 | Bacteria strains

G. amarae (NCIB 11222 strain) was purchased from NCIMB LTD.

2.2 | Materials

Reference mycolic acids from *M. bovis* were bought from Avanti Polar Lipids. Ammonium acetate was obtained from Honeywell. Potassium hydroxide, ammonium formate, acetone, hydrochloric acid and methanol (UHPLC grade) were obtained from Fisher Scientific™. Chloroform (HPLC grade) was obtained from Macron Fine Chemicals™. Nutrient broth was obtained from Oxoid Ltd. 18MΩ water was collected from Millipore S.A.S. water systems.

2.3 | Bacterial growth

Mycobacteria *G. amarae* was grown in nutrient agar and broth. A total of 20 ml liquid cultures were grown at 30°C for 1 week.

2.4 | Bacterial lipid extraction

Extractable MA isolation was achieved following Alshehry et al.[16] In brief, biomass was harvested and centrifuged (10 min, 2000 rpm). The biomass was transferred to a glass tube and freeze-dried. A total of 15 ml of 1-butanol/methanol (1:1, v:v) + 5mM ammonium formate was added, and the mixture was vortexed, sonicated (1 h) and centrifuged (10 min, 2000 rpm). The liquid layer was transferred to a round bottom flask; the previous steps were repeated twice for the biomass residue. The solid residue was reserved for saponification. The liquid was dried using a rotatory evaporator and transferred to a glass vial using chloroform and acetone rinses. These lipid extracts were dried and reconstituted in chloroform/methanol (1:2, v:v) + 5mM ammonium acetate.

The solid residue was saponified to extract MA covalently bonded to the cell wall following a method modified from Vilchèze et al.[17] Biomass residue was mixed with 2 ml of saponification reagents (methanol/water, 1:1, v:v + 25% potassium hydroxide) and heated (120°C for 1 h). Once cooled, 2 ml of chloroform and 1.5 ml of acidification reagent (hydrochloric acid/water, 1:1, v:v) were added. The chloroform layer was extracted, dried (40°C under a flow of nitrogen) and reconstituted in chloroform/methanol (1:2) + 5mM ammonium acetate.

Prior to analysis, the extractable and saponified MA extracts were combined into a total *Gordonia* mycolic acid extract. Samples were stored at −20°C until analysis.

Samples of reference mycolic acids from *M. bovis* were prepared to a concentration of 250 µg/ml in chloroform/methanol (1:2, v:v) + 5mM ammonium acetate and stored at −20°C until analysis.

2.5 | Instrumentation

All data were acquired using a SELECT SERIES Cyclic IMS mass spectrometer (Waters Corporation, Wilmslow, UK) with electrospray ionization (ESI) and by direct infusion of the sample using a syringe pump (Harvard Apparatus, Cambridge, UK) at a flow rate of 10 µl/min. MS full scan acquisitions in time-of-flight and ion mobility modes for MA from both bacteria were carried out in negative mode with the following instrument settings: capillary voltage, 2 kV; cone voltage, 40 V; source temperature, 120°C; desolvation temperature, 400°C; desolvation gas flow rate, 580 L/hour and N_2 cIM cell pressure, 1.77 mbar. The cIM separator (98 cm path length) had a resolving power (R) of ≈ 65 x (n. of passes)$^{0.5}$ ($\Omega/\Delta\Omega$).[14]

Data were acquired and processed using MassLynx software (v4.2) (Waters Corporation).

2.6 | Cyclic IM isomer separation and fragmentation

Target lipid *m/z* values were chosen based on an MS full-scan acquisition. The instrument was then switched to ion mobility enabled MS/MS mode where the quadrupole was centred on the target precursor *m/z* value with a narrow transmission window of ions (~1 *m/z* units), manual MS/MS RF ramp mode was selected and initial and final *m/z* ramp was set to 50 and 200, respectively. The following travelling wave parameters were applied: cyclic velocity and array velocities were adjusted to 375 m/s, and static height was set to 22 V.

Separation of isomers was achieved by manually increasing the number of passes of the selected ions in the cyclic ion mobility (cIM) device. Unwanted background ions were ejected from the device to improve signal-to-noise and allow higher resolving powers to be achieved with reduced interference. When multiple isomers were observed for a given precursor, each ion mobility (IM) separated isomer was further targeted using a multi-step process using IM isolation as described previously.[14] To achieve this, individual MA ions were selected by the quadrupole and passed into the cIM, individual isomer conformations were isolated within the cIM whilst the other (unwanted) conformations were ejected and discarded from the cyclic device. Following this selection, additional passes were used for further separation and the selection and ejection steps were repeated (where necessary) to fully isolate each conformation for fragmentation. If no isomer separation was observed after elevated separation times for *G. amarae* and *M. bovis* (70 and 75 passes, circa 1.5–3.5 s, respectively), no further separation or IM isolation was attempted. As the ion mobility resolving power of the instrument increases with the square root of the number of passes,[14] it would therefore require a significant increase in the number of passes required and hence resolution to observe any unresolved features. So, at this point, these analytes were considered to have only one (resolvable) conformation under the conditions employed. Finally, mass and mobility-isolated ions were fragmented by applying a post-mobility transfer collision energy between 38 and 46 V depending on the lipid carbon chain length for *G. amarae* MA, and between 65 and 75 V for *M. bovis* MA.

3 | RESULTS AND DISCUSSION

3.1 | *Gordonia amarae* MA cIM isomer separation

Mycolic acids from *G. amarae* strains are C_{31}–C_{54} (*m/z* 550–880).[18] However, not all strains of a bacterial species would be expected to

contain the same abundance of all their lipids. This is seen in Figure 1, in which the bacteria tested had the main distribution of MAs between *m/z* 715 and 830. The MAs are typically observed clustered into sets (sets (A) to (D)). The presence of ions separated by 2 *m/z* within a set corresponds to a variation in the number of double bonds within the aliphatic chains. The separation of 28 *m/z* between sets corresponds to an increase of two carbons within the aliphatic chains of the MAs. The most abundant MA species was observed at *m/z* = 771.72, found in set (C).

A survey mobility analysis was carried out on all ions in MA set (C) individually (*m/z* 769–774) to investigate the presence of possible isobaric compounds and their isomer patterns.

Two isobaric isomers were resolved from the *m/z* = 771.72 mycolic acid ion (Figure 2). Separation was initially visible after

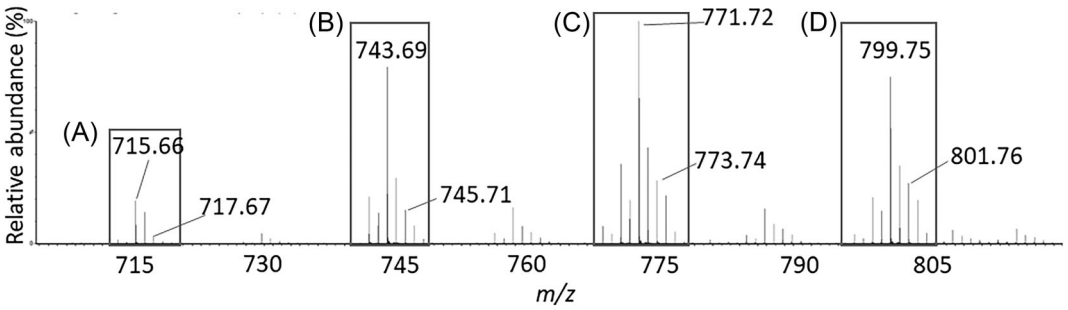

FIGURE 1 Full scan mass spectrum of *Gordonia amarae* from *m/z* 700–820; showing four main sets of mycolic acids (A) to (D).

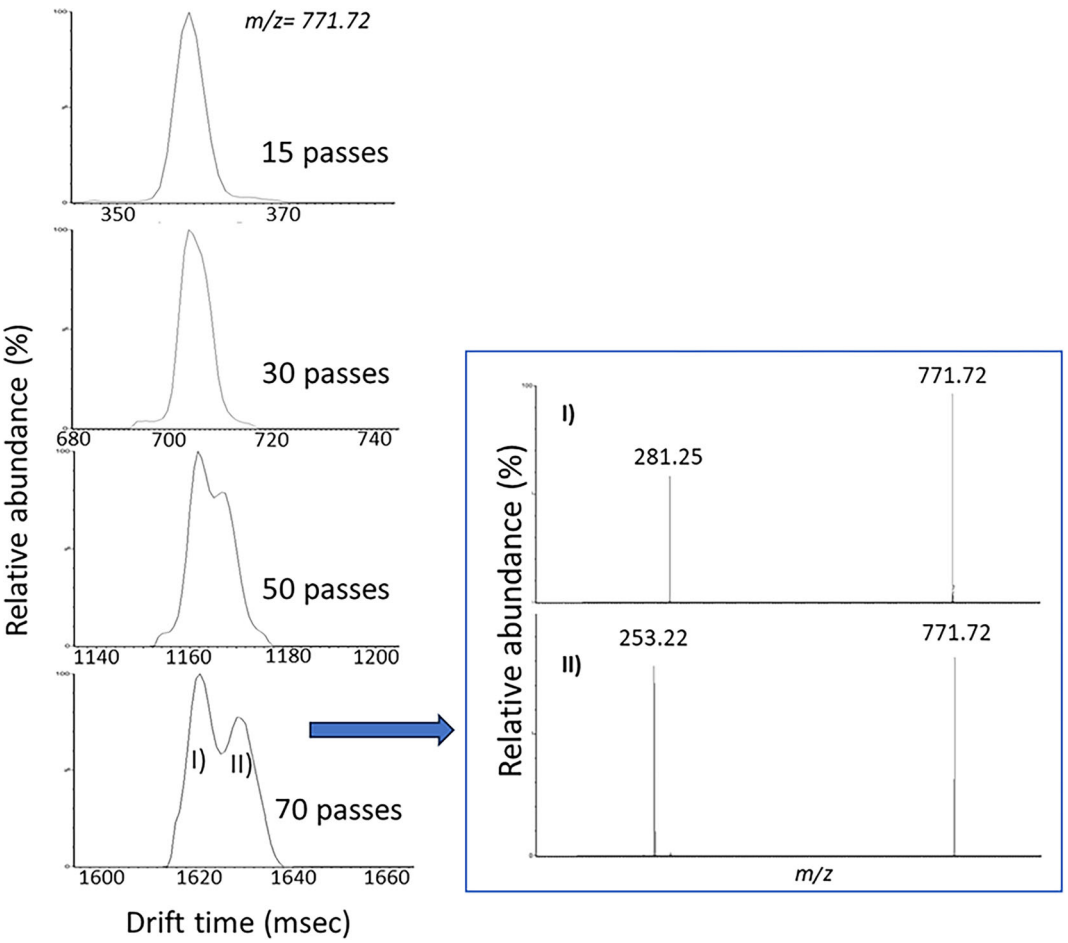

FIGURE 2 Cyclic IM separation process from 15 to 70 passes for *m/z* 771.72 mycolic acid from *Gordonia amarae*. Two isomers are observed from a single peak after 70 passes of the cyclic device. Fragmentation of the two separated peaks occurred with a transfer collision energy of 44 V (right box). [Color figure can be viewed at wileyonlinelibrary.com]

30 passes when a slight shoulder appeared. This second conformation was partially separated after 70 passes of the cyclic device, which corresponds to a resolving power of ~544 Ω/ΔΩ. Each cIM-separated peak was then post-mobility fragmented in isolation (Figure 2). The first isomer produced a main fragment at $m/z = 281.25$. The second isomer main fragment was observed at $m/z = 253.22$.

A similar analysis was conducted for +2 m/z of the most abundant ion in set (C), $m/z = 773.74$, to investigate if there was any difference compared to the most abundant ion. Three isomers were resolved after 20 passes of the cyclic device, from the initially single peak in the arrival time distribution (ATD) for the MA ion at $m/z = 773.74$ as observed in Figure 3. After 6 passes of the cIM device, a second conformation was resolved from the main peak. A third isomer was visible after 14 passes, and 3 isomers were resolved (albeit not baseline resolved) after 20 passes, corresponding to a resolving power of ~291 Ω/ΔΩ.

As the resolution is mobility-dependent, each compound and isomer requires a different separation time and hence a different number of passes. More passes were needed to separate isobaric compounds from $m/z = 771.72$ MA (70 passes) than for $m/z = 773.74$ (20 passes), in the first instance.

Beyond 20 passes, the most mobile MA isomer caught up with the least mobile ion and therefore separation was lost as the cyclic mobility device was full (wrap-around). To avoid this, each individual isomer resolved from the $m/z = 773.74$ lipid ion was isolated in the mobility device and the other conformations were discarded. Each isolated isomer was subjected to an additional 50 passes of the cyclic device (70 passes in total) and then fragmented using post-mobility transfer collision energy. As exhibited in Figure 4, other conformations (labelled (A) to (F)) were resolved from the first 3 observed peaks. Post-mobility fragmentation showed four main fragments ($m/z = 253.22$, 255.23, 281.25 and 283.26), with each individual fragment corresponding to a separate conformation. Possible structures for the fragments are proposed (Figure 4). Fragment $m/z = 253.22$ could correspond to a chemical formula of $C_{16}H_{29}O_2$ (2 unsaturations) with a mass accuracy of −6.32 ppm when the observed mass is compared to its theoretical mass. Fragment $m/z = 281.25$ could correspond to a chemical formula of $C_{18}H_{33}O_2$ (2 unsaturations) giving a mass accuracy of −6.40 ppm when the observed mass is compared to its theoretical mass; this would also correspond to the fragments observed for $m/z = 771.72$. Fragments $m/z = 255.23$ and 283.26 structures could be similar to the ones from $m/z = 253.22$ and $m/z = 281.25$, with 1 unsaturation, corresponding to $C_{16}H_{31}O_2$ and $C_{18}H_{35}O_2$, respectively. As the fragments' possible chemical formulas are within a ± 10.00 ppm limit, they can be considered a potential match.

Further analysis was done on $m/z = 773.74$ lipid ion due to the possibility that one of the mobility-separated conformations was a result of $^{13}C_2$ isotope from the most abundant ion in the set ($m/z = 771.72$) and not an isomer of $m/z = 773.74$. When the ATD of both MA ions were compared after 20 passes of the cyclic device (Figure 5), a direct overlay of $m/z = 771.72$ over the resolved peak I) from $m/z = 773.74$ was observed. After peak I) was isolated and subjected to 50 additional passes of the cyclic device (70 passes in total), and similar separation and ATD to $m/z = 771.72$ was shown. ATD comparison together with identical fragmentation patterns (Figure 2 and Figure 4) confirm that the origin of this conformation was a $m/z = 771.72$ $^{13}C_2$ isotope.

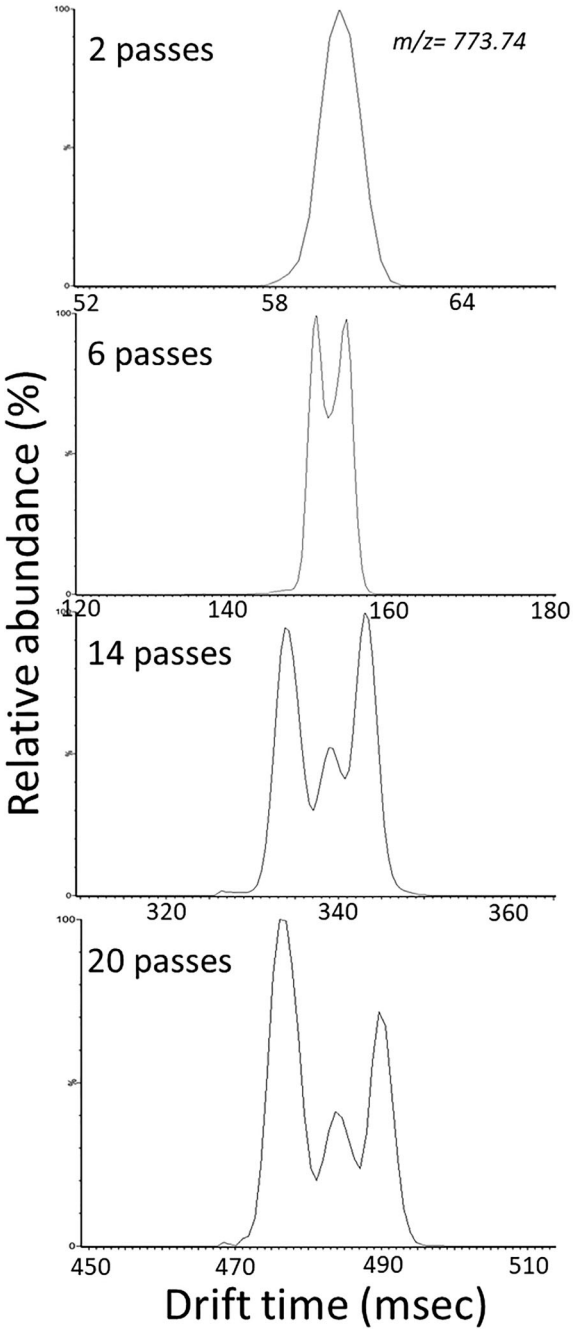

FIGURE 3 cIM separation process from 2 to 20 passes for MA m/z 773.74 from *Gordonia amarae*. Three isomers are resolved from an initial single peak.

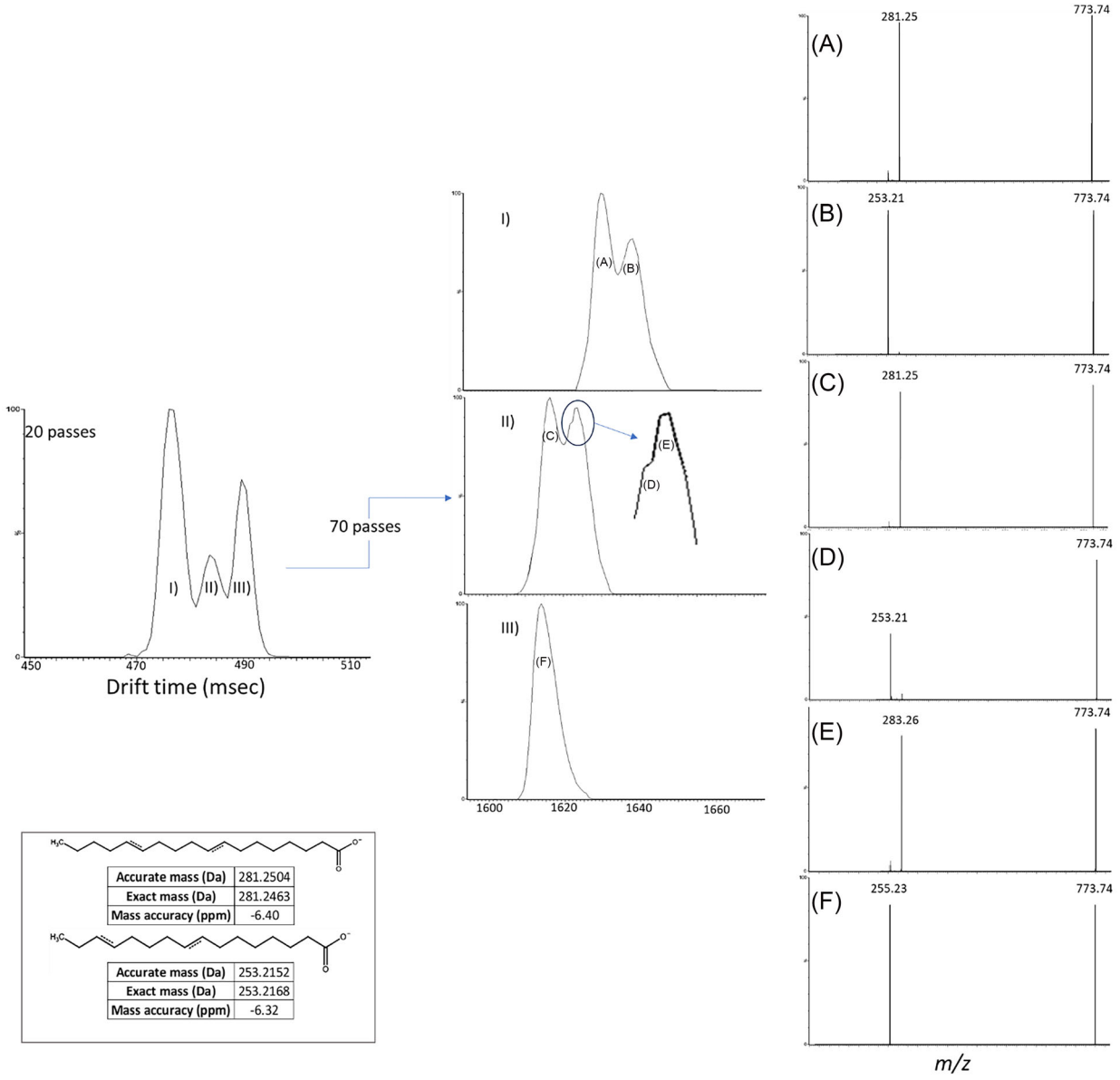

FIGURE 4 Extracted arrival time distributions (ATDs) for *m/z* 773.74 after 20 passes of the cyclic device (top left), further separation of resolved peaks I), II) and III) (middle), fragmentation of the separated peaks with a transfer collision energy of 44 V (right) and possible main fragment structures (bottom left). *Note*: The position of unsaturations cannot be determined via this method. [Color figure can be viewed at wileyonlinelibrary.com]

The remaining MA ions in set (C) (see Figure 1 for full scan) from *G. amarae* were also analysed by cIM. No further resolvable conformations were found for $m/z = 769.75$ and 770.76, (-2 *m/z* and -1 *m/z* of the most abundant ion of the set respectively). $m/z = 772.78$ ($+1$ *m/z* of the most abundant ion of the set) displayed a very similar separation and fragmentation process to $m/z = 771.72$, with two conformations separated after 70 passes of the cyclic device and $m/z = 281.25$ and 253.21 as the main fragment of the first conformation and $m/z = 253.21$ as the main fragment of the second conformation. $m/z = 774.80$ had an identical separation and fragmentation process to $m/z = 773.74$; three isomers were resolved after 20 passes and then three extra conformations were separated after 50 additional passes, with $m/z = 253.22$, 255.23, 281.25 and 283.26 fragments present. $m/z = 772.78$ and $m/z = 774.80$ are ^{13}C isotopes from $m/z = 771.72$ and $m/z = 773.74$, hence, identical separation is expected and observed.

Based on the obtained results, the most abundant ion and the ion $+2$ *m/z* within all the MA sets from *G. amarae* from $m/z = 715$ to 830 were selected for cIM isomer separation and fragmentation analysis. The results are summarized in Table 1. An ion was reported as having 1 (resolvable) conformation if no isomers were observed after 70 passes.

The most abundant ion of each set of MA has 1–2 conformations, while the MA + 2 *m/z* has 3–6 conformations. The number of passes

required for isomer separation is greater for the most abundant MA in each set than for the +2 *m/z* MA (Table 1), which suggests that isomers from the most abundant ions are structurally more similar to each other than those from +2 *m/z*. *m/z* = 281.25 and 253.22 were the main fragments present in all lipid ions. Fragments *m/z* = 255.23 and 283.26 fragments were also present in some lipid isomer confrontations from +2 *m/z* MA, although not always simultaneously. These distinctive isomer patterns could provide potential biomarker targets to identify the presence of *G. amarae* in wastewater treatment plants.

3.2 | *Mycobacterium bovis* MA cyclic IM isomer separation

The same process was applied to *M. bovis* as a comparison to MA lipids in *G. amarae*. *M. bovis* MA are C_{75} – C_{91} and therefore are found

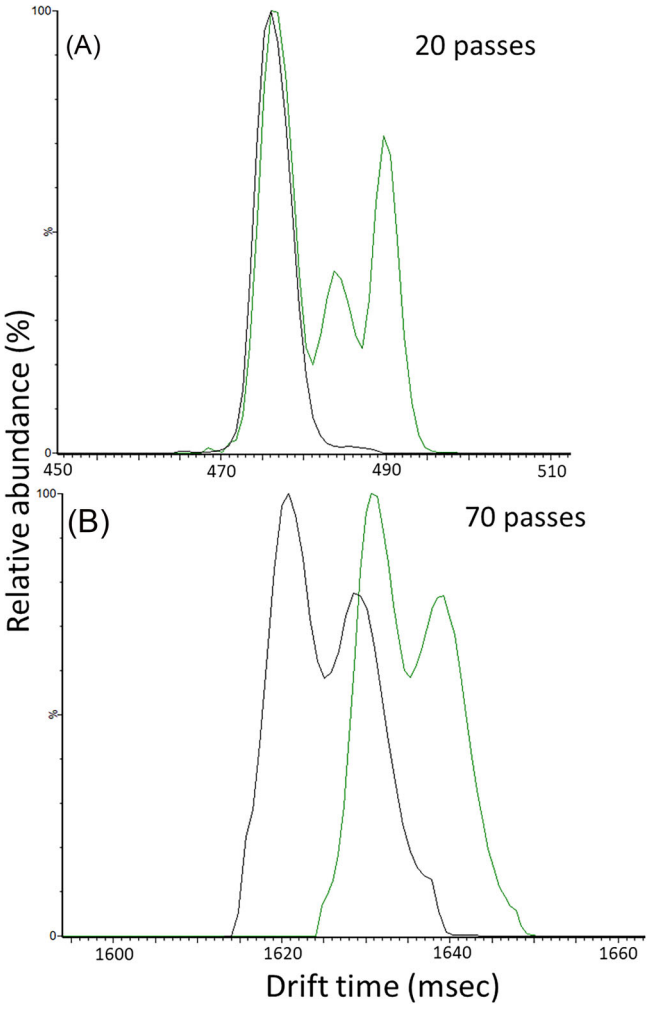

FIGURE 5 ATDs comparison of MA *m/z* = 771.72 (black) and *m/z* = 773.74 (green) from *Gordonia amarae* after 20 passes of the cyclic device (A)), and ATDs comparison of MA *m/z* = 771.72 (black) and isolated ion mobility separated peak I) from *m/z* = 773.74 (green), after 70 passes of the cyclic device (B)). [Color figure can be viewed at wileyonlinelibrary.com]

TABLE 1 Mycolic acid isomers observed in *Gordonia amarae*. The most abundant ion of each set of MA was marked with *.Predicted chemical formulas for MA ions with at least one ^{13}C were marked with **. Number of double bonds for predicted chemical formulas include unsaturations and C=O from acid and keto groups. Where multiple fragments were present, the most abundant fragment was underlined. If isolation and further separation were required to show other conformations, these were denoted as conformation X.2 and X.3.

Lipid ion observed mass	Predicted formula	Mass accuracy (ppm)	n° of double bonds	MA group	n° of conformations	n° of passes	Transfer CE (V)	Fragments *m/z*					
								Conf. 1		Conf. 2			Conf. 3
								1.1	1.2	2.1	2.2	2.3	
715.6593*	$C_{47}H_{87}O_4$	−1.59	4	a)	1	70	38	253 + 281					
717.6736	$C_{47}H_{89}O_4$	−3.46	3		3	70	42	253 + 281		253			255
743.6932*	$C_{49}H_{91}O_4$	1.97	4	b)	2	70	40	281	253				
745.7065	$C_{49}H_{93}O_4$	−1.19	3		6	70	42	281	253	281	253	283	255
769.7081	$C_{51}H_{93}O_4$	0.93	5	c)	1	70	42	253 + 281					
770.7095	$^{**}C_{51}H_{93}O_4$				1	70	42	253 + 281					
771.7237*	$C_{51}H_{95}O_4$	0.86	4		2	70	44	281	253				
772.7264	$^{**}C_{51}H_{95}O_4$				2	70	45	281	253				
773.7379	$C_{51}H_{97}O_4$	−1.02	3		6	70	44	281	253	281	253	283	255
774.7418	$^{**}C_{51}H_{97}O_4$				6	70	44	281	253	281	253	283	255
799.7542*	$C_{53}H_{99}O_4$	−0.17	4	d)	2	70	42	281	253				
801.7630	$C_{53}H_{101}O_4$	−8.71	3		6	70	46	281	253	281	253	283	255

between m/z = 1,090 and 1,300. They are composed of three MA classes: alpha, keto and methoxy.[7] Two sets from each class of mycolic acids were selected for analysis from an MS full-scan spectrum (Figure 6). As with the previous analysis of *G. amarae*, the most abundant ion of each set and those with 2 m/z greater than the most abundant ion were chosen for cIM analysis.

Analysis was performed following the same methods applied to MA lipids in *Gordonia amarae* (Figure 7). As MA from *M. bovis* is larger than the MA from *G. amarae*, a longer analysis was required. All selected MA from *M. bovis* were analysed with 75 passes of the cyclic device, corresponding to a resolving power of ~563 Ω/ΔΩ.

cIM analysis from alpha (sets (A) and (B)) and methoxy (sets (E) and (F)) MA did not resolve any conformations during the separation process, as seen in Figure 7 for m/z = 1136.17 (alpha) and 1252.29 (methoxy), suggesting no isobaric compounds could be resolved under the applied conditions. Two conformations were separated from keto-MA (sets (C) and (D)). For example, in m/z = 1236.26 (Figure 7; Table 2), a shoulder was visible after

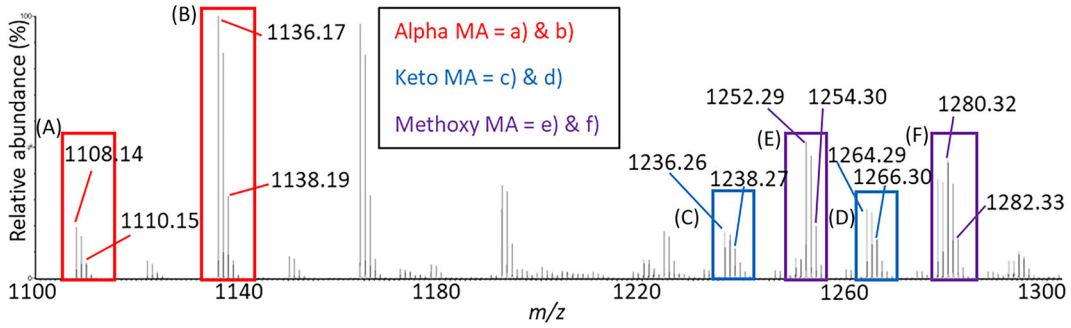

FIGURE 6 Full mass spectrum of reference mycolic acids from *Mycobacterium bovis*, showing the three different classes of MA. [Color figure can be viewed at wileyonlinelibrary.com]

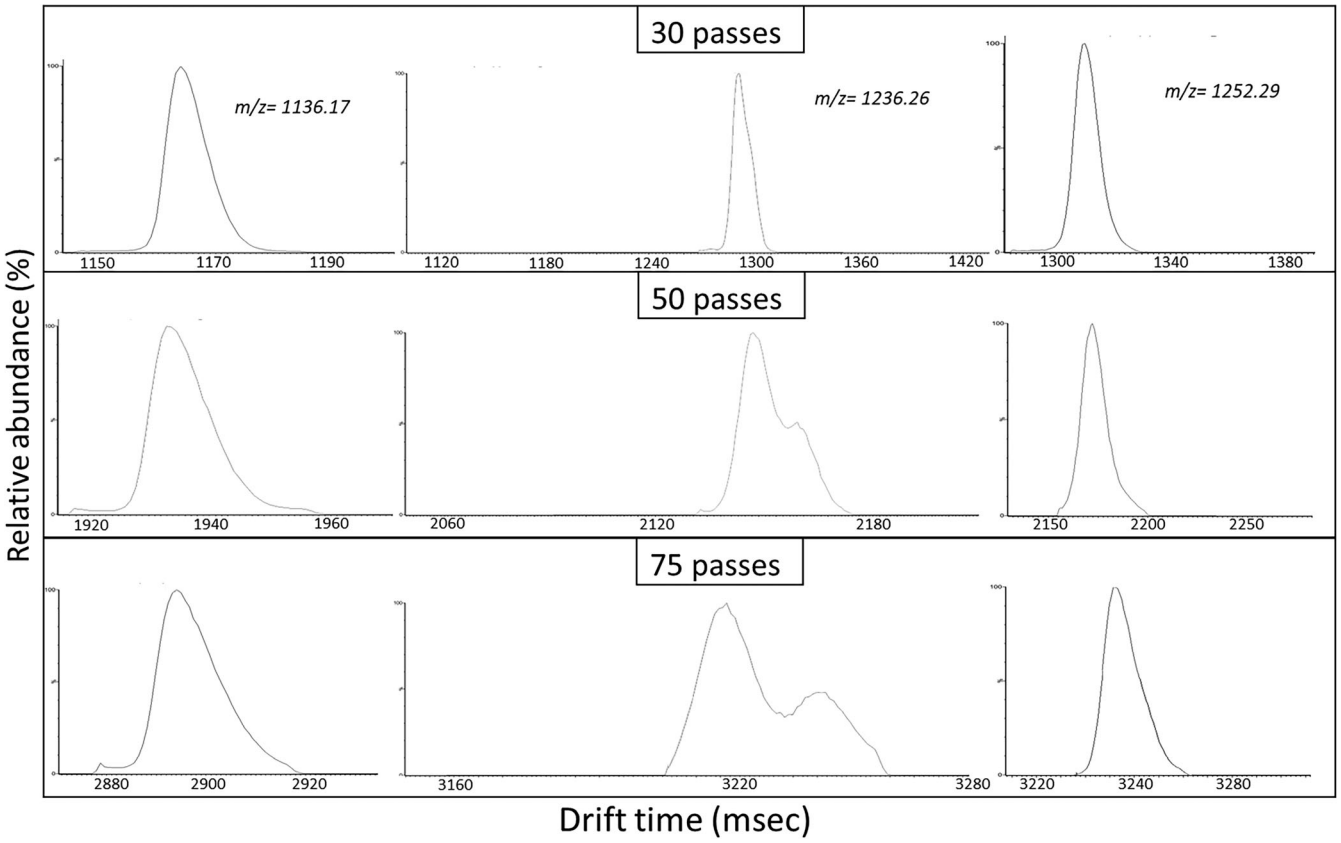

FIGURE 7 Cyclic IM separation process from 30 to 75 passes for m/z 1136.17 (left), 1236.26 (middle) and 1252.29 (right) alpha, keto and methoxy mycolic acids, respectively, from *Mycobacterium bovis*.

TABLE 2 MA isomers resolved from *Mycobacterium bovis* after 75 passes of the cyclic device. The most abundant ion of each set of MA was marked with *. Number of double bonds for predicted chemical formulas include unsaturations and C=O from acid and keto groups. Where multiple fragments were present, the most abundant fragment was underlined.

Lipid ion observed mass	Predicted formula	Mass accuracy (ppm)	n° of double bonds	Lipid class	n° of conformations	n° of passes	Transfer CE (V)	Fragments *m/z*	
								Conf. 1	Conf. 2
1108.1356*	$C_{76}H_{147}O_3$	0.52	3	Alpha	1	75	65	367 + 395	
1110.1504	$C_{76}H_{149}O_3$	−0.25	2	Alpha	1	75	65	367 + 396	
1136.1705*	$C_{78}H_{151}O_3$	3.68	3	Alpha	1	75	65	367 + 395	
1138.1862	$C_{78}H_{153}O_3$	3.71	2	Alpha	1	75	65	367 + 395	
1236.2562*	$C_{84}H_{163}O_4$	0.86	3	Keto	2	75	70	367 + 395	367 + 395
1238.2683	$C_{84}H_{165}O_4$	−2.01	2	Keto	2	75	70	367 + 395	395
1252.2897*	$C_{85}H_{167}O_4$	2.6	2	Methoxy	1	75	70	367 + 395	
1254.3032	$C_{85}H_{169}O_4$	0.89	1	Methoxy	1	75	70	367 + 395	
1264.2874*	$C_{86}H_{167}O_4$	0.76	3	Keto	2	75	70	395	395
1266.3054	$C_{86}H_{169}O_4$	2.61	2	Keto	1	75	70	395	
1280.3174*	$C_{87}H_{171}O_4$	−0.26	2	Methoxy	1	75	75	395	
1282.3325	$C_{87}H_{173}O_4$	−0.69	1	Methoxy	1	75	75	395	

50 passes of the cyclic device and two isomers were partially resolved after 75 passes, although they were not baseline resolved.

Three different MA (*m/z* = 1136.17, 1236.26 and 1252.29) were fragmented, including each individually resolved isomer for *m/z* = 1236.26. A similar analysis was performed for the other selected MA (Figure 6), and results collected in Table 2. The fragment *m/z* = 395.38 is present in all MA. An additional *m/z* = 367.35 fragments was also observed in the MA analytes that have a parent mass less than *m/z* = 1,254; it is the most abundant fragment in the two measured MA with a parent mass less than *m/z* = 1,136.

Fragment *m/z* = 395.38 could correspond to a chemical formula of $C_{26}H_{51}O_2$ with a mass accuracy of −1.03 ppm when the observed mass is compared to its theoretical mass. Fragment *m/z* = 367.35 could correspond to a chemical formula of $C_{24}H_{47}O_2$ giving a mass accuracy of −3.28 ppm when the observed mass is compared to its theoretical mass. As both fragments' possible chemical formulas are within a ± 10.00 ppm limit, they can be considered a potential match.

The chemical formulae shown in Table 2 for observed mycolic acids are derived from their mass accuracies, which are within ± 5 ppm limit for parent ions and can therefore be considered a potential match. Future research could include the addition of thin-layer chromatography (TLC) to explore mycolic acid decoration diversity.

Ion mobility analysis of a wider range of parent masses from *M. bovis* and closely related species could reveal whether this pattern holds more widely, thus providing insight into biosynthetic pathways of these lipids and potentially into lipid-targeting medical treatments. Future work could also extend cIM analysis to other mycobacteria, such as *Mycobacterium smegmatis*, *Mycobacterium tuberculosis* H37Rv and other non-tuberculous mycobacterium.

4 | CONCLUSION

Mycolic acid (MA) isomers from the foaming-related bacteria *G. amarae* and pathogenic bacteria *M. bovis* were successfully resolved from lipid ions that appeared as single peaks in a full scan mass spectrum. This was achieved by individually targeting the most abundant ions within each set of MA, as well as the ion 2 *m/z* higher, with the quadrupole and performing multiple passes of the cyclic ion mobility device. Not only did this allow separation of previously unresolved isomers, it additionally allowed fragmentation of each conformation separately. The patterns of isomerization and fragmentation varied between the two bacterial species, potentially suggesting biosynthetic differences. This technique offers the possibility to obtain a higher level of separation to get an improved lipidomic characterization, which could help future projects in the analysis and understanding of lipids isomers from vital bacteria. Results obtained in this study from *G. amarae* and *M. bovis* could aid in designing foaming prevention processes and in understanding how isomers could be used for the development of new anti-tuberculosis drugs, respectively.

AUTHOR CONTRIBUTIONS

Hector de las Heras Prieto: Investigation; writing—original draft; methodology; writing—review and editing; formal analysis; validation; data curation. **Laura Cole M:** Investigation; writing—review and editing; supervision. **Sarah Forbes:** Investigation; writing—review and editing; supervision. **Martin Palmer:** Investigation; writing—review and editing; methodology; software. **Rachel Schwartz-Narbonne:** Conceptualization; investigation; funding acquisition; writing—review and editing; supervision.

ACKNOWLEDGMENTS

BMRC technical team, especially Michael Cox, Jonathan Foster and Jef Clark, as well as Scott Hardy and Matt Gentry, are thanked for laboratory support. Rachel Schwartz-Narbonne was supported by the Community for Analytical Measurement Science through a 2021 CAMS ECR Fellowship Award funded by the Analytical Chemistry Trust Fund (https://cams-uk.co.uk|https://twitter.com/cams_uk|www.linkedin.com/company/cams-uk) and a BMRC graduate teaching assistant scholarship.

CONFLICT OF INTEREST STATEMENT

Martin Palmer is an employee of Waters Corporation who manufacture and sell mass spectrometers incorporating the technology described above.

Hector de las Heras Prieto, Laura M Cole, Sarah Forbes and Rachel Schwartz-Narbonne declare no conflicts of interest.

PEER REVIEW

The peer review history for this article is available at https://www.webofscience.com/api/gateway/wos/peer-review/10.1002/rcm.9917.

DATA AVAILABILITY STATEMENT

The data that support the findings of this study are available from the corresponding author upon reasonable request.

ORCID

Hector de las Heras Prieto https://orcid.org/0000-0002-4194-8207
Martin Palmer https://orcid.org/0000-0003-1658-9334

REFERENCES

1. Batt SM, Minnikin DE, Besra GS. The thick waxy coat of mycobacteria, a protective layer against antibiotics and the host's immune system. *Biochem J*. 2020;477(10):1983-2006. doi:10.1042/BCJ20200194
2. Tuberculosis (TB). https://www.who.int/news-room/fact-sheets/detail/tuberculosis
3. Pagilla KR, Sood A, Kim H. Gordonia (nocardia) amarae foaming due to biosurfactant production. *Water Sci Technol*. 2002;46(1-2):519-524. doi:10.2166/wst.2002.0528
4. Nataraj V, Varela C, Javid A, Singh A, Besra GS, Bhatt A. Mycolic acids: deciphering and targeting the Achilles' heel of the tubercle bacillus. *Mol Microbiol*. 2015;98(1):7-16. doi:10.1111/mmi.13101
5. Marrakchi H, Lanéelle MA, Daffé M. Mycolic acids: structures, biosynthesis, and beyond. *Chem Biol*. 2014;21(1):67-85. doi:10.1016/j.chembiol.2013.11.011
6. Zhao J, Siddiqui S, Shang S, et al. *Mycolic acid-specific T cells protect against Mycobacterium tuberculosis infection in a humanized transgenic mouse model*. eLife; 2015.
7. Naicker B. Identification of mycolic acid class ratios from Mycobacterium species using liquid chromatography-mass spectrometry. 2019.
8. Jackson M, McNeil MR, Brennan PJ. Progress in targeting cell envelope biogenesis in mycobacterium tuberculosis. *Future Microbiol*. 2013;8(7):855-875. doi:10.2217/fmb.13.52
9. Nishiuchi Y, Baba T, Yano I. Mycolic acids from Rhodococcus, Gordonia, and Dietzia. *J Microbiol Methods*. 2000;40(1):1-9. doi:10.1016/S0167-7012(99)00116-5
10. Smit NT, Villanueva L, Rush D, et al. Novel hydrocarbon-utilizing soil mycobacteria synthesize unique mycocerosic acids at a Sicilian everlasting fire. *Biogeosciences*. 2021;18(4):1463-1479. doi:10.5194/bg-18-1463-2021
11. Liu Y, Kaffah N, Pandor S, Sartain MJ, Larrouy-Maumus G. Ion mobility mass spectrometry for the study of mycobacterial mycolic acids. *Sci Rep*. 2023.
12. Dodds JN, Baker ES. Ion mobility spectrometry: fundamental concepts, instrumentation, applications, and the road ahead. *J am Soc Mass Spectrom*. 2019;30(11):2185-2195. doi:10.1007/s13361-019-02288-2
13. Pringle SD, Giles K, Wildgoose JL, et al. An investigation of the mobility separation of some peptide and protein ions using a new hybrid quadrupole/travelling wave IMS/oa-ToF instrument. *Int J Mass Spectrom*. 2007;261(1):1-12. doi:10.1016/j.ijms.2006.07.021
14. Giles K, Ujma J, Wildgoose J, et al. A cyclic ion mobility-mass spectrometry system. *Anal Chem*. 2019;91(13):8564-8573. doi:10.1021/acs.analchem.9b01838
15. Riches E, Palmer ME. Application of a novel cyclic ion mobility-mass spectrometer to the analysis of synthetic polymers: a preliminary evaluation. *Rapid Commun Mass Spectrom*. 2020;34(S2). doi:10.1002/rcm.8710
16. Alshehry ZH, Barlow CK, Weir JM, Zhou Y, McConville MJ, Meikle PJ. An efficient single phase method for the extraction of plasma lipids. *Metabolites*. 2015;5(2):389-403. doi:10.3390/metabo5020389
17. Vilchèze C, Jacobs WR. Isolation and analysis of mycobacterium tuberculosis mycolic acids. *Curr Protoc Microbiol*. 2007;5(1). doi:10.1002/9780471729259.mc10a03s05
18. Stratton HM, Brooks PR, Seviour RJ. Analysis of the structural diversity of mycolic acids of Rhodococcus and Gordonla isolates from activated sludge foams by selective ion monitoring gas chromatography–mass spectrometry (SIM GC–MS). *J Microbiol Methods*. 1999;35(1):53-63. doi:10.1016/S0167-7012(98)00102-X

How to cite this article: de las Heras Prieto H, Cole LM, Forbes S, Palmer M, Schwartz-Narbonne R. Separation of mycolic acid isomers by cyclic ion mobility-mass spectrometry. *Rapid Commun Mass Spectrom*. 2024;38(23):e9917. doi:10.1002/rcm.9917